Mechanism of Silver Nanoparticle Toxicity Is Dependent on Dissolved Silver and Surface Coating in Caenorhabditis elegans

ARTICLE *in* ENVIRONMENTAL SCIENCE & TECHNOLOGY · DECEMBER 2011

Impact Factor: 5.33 · DOI: 10.1021/es202417t · Source: PubMed

7 AUTHORS, INCLUDING:

Xinyu Yang
Duke University
12 PUBLICATIONS **479** CITATIONS
SEE PROFILE

Andreas Gondikas
University of Vienna
13 PUBLICATIONS **516** CITATIONS
SEE PROFILE

Stella Marinakos
Duke University
28 PUBLICATIONS **1,875** CITATIONS
SEE PROFILE

Environmental Science & Technology

Article

pubs.acs.org/est

Mechanism of Silver Nanoparticle Toxicity Is Dependent on Dissolved Silver and Surface Coating in *Caenorhabditis elegans*

Xinyu Yang,[†] Andreas P. Gondikas,[‡] Stella M. Marinakos,[‡] Melanie Auffan,[§] Jie Liu,[‡,∥] Heileen Hsu-Kim,[‡] and Joel N. Meyer*,[†]

[†]Nicholas School of the Environment and Center for the Environmental Implications of Nanotechnology, Duke University, Durham, North Carolina 27708-0328, United States

[‡]Department of Civil & Environmental Engineering and Center for the Environmental Implications of Nanotechnology, Duke University, Durham, North Carolina 27708, United States

[§]CEREGE UMR 6635 CNRS Aix-Marseille Univ, iCEINT international Consortium for the Environmental Implications of NanoTechnology, 13545 Aix en Provence, France

[∥]Department of Chemistry, Duke University, Durham, North Carolina 27708, United States

Supporting Information

ABSTRACT: The rapidly increasing use of silver nanoparticles (Ag NPs) in consumer products and medical applications has raised ecological and human health concerns. A key question for addressing these concerns is whether Ag NP toxicity is mechanistically unique to nanoparticulate silver, or if it is a result of the release of silver ions. Furthermore, since Ag NPs are produced in a large variety of monomer sizes and coatings, and since their physicochemical behavior depends on the media composition, it is important to understand how these variables modulate toxicity. We found that a lower ionic strength medium resulted in greater toxicity (measured as growth inhibition) of all tested Ag NPs to *Caenorhabditis elegans* and that both dissolved silver and coating influenced Ag NP toxicity. We found a linear correlation between Ag NP toxicity and dissolved silver, but no correlation between size and toxicity. We used three independent and complementary approaches to investigate the mechanisms of toxicity of differentially coated and sized Ag NPs: pharmacological (rescue with trolox and N-acetylcysteine), genetic (analysis of metal-sensitive and oxidative stress-sensitive mutants), and physicochemical (including analysis of dissolution of Ag NPs). Oxidative dissolution was limited in our experimental conditions (maximally 15% in 24 h) yet was key to the toxicity of most Ag NPs, highlighting a critical role for dissolved silver complexed with thiols in the toxicity of all tested Ag NPs. Some Ag NPs (typically less soluble due to size or coating) also acted via oxidative stress, an effect specific to nanoparticulate silver. However, in no case studied here was the toxicity of a Ag NP greater than would be predicted by complete dissolution of the same mass of silver as silver ions.

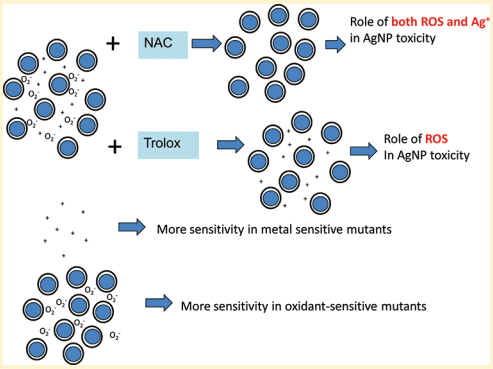

INTRODUCTION

The increased use of silver nanoparticles (Ag NPs) as antimicrobial agents in commercial and medical products has led to elevated human and environmental exposures.[1−3] In addition to being bacteriocidal,[4−7] Ag NPs are toxic to other taxa. Documented effects include developmental deformities in zebrafish,[8−10] altered stress-related gene expression in Japanese medaka,[11] respiratory stress in Eurasian perch,[12] mitochondrial toxicity in human cells,[13] inflammatory responses in rats,[14] neurotoxicity in mice,[15] and decreased growth and reproductive capacity in *Caenorhabditis elegans*.[16,17]

Despite many recent publications on Ag NP toxicity, the mechanism of Ag NP toxicity remains unclear.[18] Understanding this mechanism is critical for risk assessment; if Ag NP toxicity is driven by release of dissolved silver, our current knowledge relating dissolved silver speciation and toxicity may be highly informative for risk assessment. If on the other hand Ag NPs have unique toxicities deriving from their nanoparticulate form, additional studies will be required. Release of metal ion from nanoparticle dissolution is an important mechanism for toxicity of some NPs,[19] and recent work has suggested that oxidative dissolution rates of Ag NPs may be quite high under some circumstances.[20] Several studies suggest that the mechanism of Ag NP toxicity is largely explained by Ag ions (Ag^+). For example, no toxicity was observed when Ag^+ was complexed by a thiol ligand.[8,21−25] Using genetic analysis, we also found evidence that Ag NP toxicity was mediated by ionic silver release.[17] However, other studies suggest that ion release does not explain all toxicity, and some support a role for generation of reactive oxygen species (ROS),

Received: July 15, 2011
Revised: November 29, 2011
Accepted: December 7, 2011
Published: December 7, 2011

which might occur at the surface of Ag NPs[26−30] but is not expected to result from silver ion dissolution alone. One study reported that cysteine, a strong Ag^+ ligand, only partially rescued Ag NP toxicity,[31] while others found that Ag NP cytotoxicity was independent of Ag^+ concentration and resulted primarily from oxidative stress.[28,32] Thus, the reported mechanism of Ag NP toxicity has been variable depending on the Ag NP and system in question and needs further elucidation, preferably using multiple different Ag NPs that might have different mechanisms of action, but all measured in the same system.

Ag NPs have a high tendency to aggregate and are typically synthesized with surface coatings to stabilize them in suspension.[33,34] Both aggregation and surface coatings can alter Ag NP toxicity.[35] For example, biogenic Ag NPs (coated with protein) were more toxic than chemically synthesized Ag NPs, and citrate-coated Ag NPs were more toxic than PVP-coated Ag NPs.[36] However, more information on the impact of surface coatings on the mechanisms of Ag NP toxicity is needed, especially in conjunction with characterization of the physicochemical state of the particles at the time of exposure, which is critical but relatively rarely done.[20,37−40]

The goal of this study, therefore, was to investigate the factors determining Ag NP toxicity in the model organism *C. elegans*. We compared the toxicity of several sizes of Ag NPs (from 5 to 75 nm mean diameter) coated in different ways and suspended in two different culture media chosen on the basis of differing ionic strengths. We used pharmacological rescue (trolox and N-acetylcysteine), genetic knockouts (analysis of metal- sensitive and oxidative stress-sensitive mutants), and physicochemical characterization (analysis of aggregation, surface charge, crystalline structure, and dissolution of Ag NPs) to test for the importance of dissolved silver vs Ag NP-mediated oxidative stress. The use of differentially coated Ag NPs of similar size permitted insight into the role of coating.

MATERIALS AND METHODS

C. elegans Strains and Culture. *C. elegans* were cultured in Petri dishes on K-agar seeded with OP50 strain *Escherichia coli*[41] to prepare nematodes for liquid medium exposure, which was carried out in 96 well plates as previously described[17] except as detailed below. In addition to wild-type, mutant strains were chosen based on their known sensitivity to certain mechanisms of toxicity. Strains N2 (wild-type Bristol), VC433 (*sod-3* deletion), TM1748 (*pcs-1* deletion, outcrossed 6 times), and TK22 (*mev-1*, mutation uncertain, outcrossed 5 times) were obtained from the *Caenorhabditis* Genetics Center (CGC; Minneapolis, MN, USA). Strain JF23 (*mtl-2* deletion, outcrossed 4 times from the VC128 strain) was a generous gift from J. Freedman and W. Boyd (NIEHS).

Ag NP Synthesis and Characterization in Stock Solution. We used 5 types of previously characterized Ag NPs: citrate-coated Ag NPs (herein referred to as "CIT_7", where the subscript indicates monomer diameter in nanometers),[17] small and large polyvinylpyrrolidone (PVP) -coated Ag NPs ("PVP_S" and "PVP_L") acquired from NanoAmor,[17] and gum arabic (GA)-coated Ag NPs ("GA_5", "GA_{22}").[42] We also manufactured two additional PVP-coated particles ("PVP_8" and "PVP_{38}"). Silver nitrate and sodium borohydride were purchased from Sigma-Aldrich. PVP with molecular weights (MW) 10,000 and 55,000, and ethylene glycol were acquired from Fisher Scientific. Ultrapure water (Barnstead NANOpure Diamond) was used in all syntheses. To synthesize the PVP-coated 8 nm Ag NPs (PVP_8), 1.5 g of PVP (MW 10,000) was dissolved in 280 mL of water in an Erlenmeyer flask. Nine mL of 0.1 M silver nitrate was added, and the solution was stirred for 5 min before adding 11 mL of ice-cold sodium borohydride (0.08 M) all at once. The PVP-stabilized silver nanoparticles were centrifuged for 3 h at 112,000*g* (Beckman Optima L-100XP equipped with a Type 45 Ti rotor). The precipitate, containing the 8 nm Ag nanoparticles, was resuspended in water. There was no detectable effect of the molecular weight of PVP on toxicity when comparing 8 nm PVP-coated Ag NPs with either 10K or 55K PVP (data not shown).

To synthesize the PVP-coated 38 nm Ag NPs (PVP_{38}), 20 g of PVP (MW 55,000) was dissolved in 50 mL of ethylene glycol. The solution was transferred to a round-bottom flask equipped with a condenser, 1.5 g of silver nitrate was added, and the mixture was stirred at room temperature. Once silver nitrate was dissolved, the solution was heated in an oil bath to 120 °C for 24 h. The PVP-stabilized silver nanoparticles were then removed from heat, diluted 1:10 with water, and purified by dialysis (Optiflux F200NR Fresenius Polysulfone Dialyzer, Fresenius Medical Care).[43,44]

The syntheses of GA_5 and GA_{22} were described by Yin et al.[42] The morphology and particle size distributions of PVP and GA-coated Ag NPs were determined using a Tecnai G2 Twin transmission electron microscopy (FEI, Hillsboro, OR) at acceleration voltages of 160 kV and 200 kV, respectively. Samples were prepared by placing a drop of the nanoparticle suspension on a standard copper grid and drying at room temperature. The UV−vis absorbance spectra of nanoparticles were acquired using a Cary 500 scan UV−vis-NIR spectrophotometer (Varian, CA). Hydrodynamic diameters of the particles were quantified by dynamic light scattering (DLS) conducted with an ALV-CGS 3 compact goniometer system (ALV-GmbH, Germany) using a helium−neon laser (λ = 632.8 nm) scattered at 90°.

COPAS Biosort Flow Sorting System and Growth Assay. The 3-day growth assay was modified from our previous protocol[17,45] and is described in more detail in Supplemental Data File 1.

Quantification of Ag NP Properties and Dissolved Silver, NAC, Borate, PVP, and Citrate Concentrations in Exposure Medium. Barnstead Nanopure-grade water (>17.8 MΩ-cm, Sigma Aldrich) was used to prepare all reagents and samples for measurements of Ag NP hydrodynamic diameter, electrophoretic mobility (and ζ-potential), and dissolved silver and N-Acetylcysteine (NAC). Trace-metal grade HNO_3 was used to adjust the pH of solutions. Ultrahigh purity nitrogen was utilized to degas reagent water for the NAC stock solutions. Borosilicate glass containers for reagents were acid cleaned by an overnight soak in 1 N HCl followed by three rinses with Nanopure water. Quantification of NAC, borate, PVP, citrate, and total silver are described in Supplemental Data File 1.

The hydrodynamic diameter of the Ag NPs was quantified by diluting an aliquot of the Ag NP stock suspension in EPA water to reach a final silver concentration ranging from 20 to 46 μM Ag. A subset of the solutions contained 123 μM NAC. This NAC concentration was 2 times higher than that used in the toxicity test exposure, due to the fact that most Ag NP concentrations in this characterization were higher than the dosing concentrations. Size and ζ potential of Ag NPs were analyzed by dynamic light scattering (DLS) (Malvern Zetasizer). Experiments with PVP-coated nanoparticles were prepared in glass containers and transferred to a 1-cm glass cuvette before analysis with DLS. The intensity-weighted average hydrodynamic diameter of the colloids was quantified over time using

incident light (λ = 633 nm) scattered at 173°. Electrophoretic mobility at 25 °C (Malvern Zetasizer) was measured in triplicate after one hour in suspension. Zeta potential was calculated from the electrophoretic mobility based on the Smoluchowski equation.[46]

Dissolution of silver and adsorption of NAC on Ag NPs were quantified to investigate how toxicity might be related to silver ion release from the NPs, and whether NAC was sorbing to the particles and influencing aggregation. Batch experiments were carried out by suspending Ag NPs in EPA water with or without NAC under ambient laboratory conditions. Replicates of the suspensions were incubated at room temperature for 1, 5, and 24 h. At each time point, a sample replicate was sacrificed for filtration using a 0.025 μm membrane filter (VSWP Millipore) inserted in a glass vacuum filtration apparatus. The filtered samples were acidified with 2% v/v HNO_3 and 0.5 v/v % HCl and allowed to digest at room temperature for at least one day prior to silver concentration quantification by ICP-MS. NAC concentration was measured in the filtrate by derivatization with DTNP and quantification by reverse phase high performance liquid chromatography (Varian ProStar).[47,48] In all Ag NP solutions, at least 65% of the initial NAC was observed in the water after filtration (Figure S1), and in all cases, the nominally dissolved NAC concentration (i.e., in filtered water) was greater than the nominally dissolved Ag concentration.

Control experiments were performed to confirm that free NAC, Ag^+, and Ag-NAC complexes were not sorbing to the filters. In these experiments, two solutions comprising 123 μM NAC and 37 μM $AgNO_3$+123 μM NAC in EPA water were filtered with the 0.025 μm membrane filters. A third solution consisting of 1.85 μM $AgNO_3$ in a $NaHCO_3$ (pH 8.3) was also prepared as the Ag^+ control. The percentage of total NAC quantified in the filtrate was 96.9% in the NAC-only mixture and 92.3% in the $AgNO_3$+NAC mixture. The recovery of total silver in the $AgNO_3$-bicarbonate mixture and $AgNO_3$+NAC mixture were 94.1% and 96.1%, respectively. The efficiency of the filtration system to remove particles was also tested by quantifying the retention of silver after filtration of Ag NP stock solutions. Filtration of the stocks resulted in removal of 99.7%, 79.5%, 99.4%, 89.7%, and 95.6% of total silver from CIT_7, GA_5, GA_{22}, PVP_8, and PVP_{38} stock suspensions, respectively. Although the monomer diameters for some of our stock suspensions were below the nominal filter pore size, particles were probably aggregated to some extent since hydrodynamic diameters (quantified by DLS) were greater than monomer diameter (quantified by TEM) for all particles. Hydrophobic or electrostatic interactions between particles and the mixed cellulose esters hydrophilic membrane may have also contributed to retention of particles during filtration.

Silver Speciation by X-ray Absorption Spectroscopy. Silver K-edge (25.514 KeV) XANES experiments (X-ray absorption near edge structure) were acquired at the European Synchrotron Radiation Facility (ESRF, France) on the FAME beamline (BM30b) with Si(220) monochromator crystals.[49,50] Samples were cooled to a temperature close to that of liquid Helium (around 10 K) during spectra acquisition into fluorescence mode using a multichannel fluorescence detector. Two samples were analyzed: bacteria alone and *C. elegans* (age-synchronized L1s) incubated with bacteria, both exposed to 1.2 μM $AgNO_3$ in EPA water. After 48 h, both bacteria and nematodes were rinsed 3 times with EPA water and centrifuged at 2200 and 5000 rpm for nematodes and bacteria, respectively. Samples were freeze-dried, homogenized, mixed with boron nitride, and pressed into thin pellets for XANES analysis. Four scans were collected for each sample. The XANES data were obtained after performing standard procedures for pre-edge subtraction and normalization using the iFEFFit software package.[51]

Data Processing and Statistical Analysis. Data from the Biosort for each aspiration time was graphed as a scatterplot between TOF and EXT, which are highly correlated values (Figure S2 and Supplemental Data File 2). As other COPAS toxicology researchers have shown, EXT values are preferable because nematode curling leads to greater variability in TOF values.[52,53] Therefore, we used EXT values for graphical presentation and statistical analysis. To exclude measurements of objects other than nematodes (e.g., Ag NP aggregates), values were deleted if they deviated by >one standard deviation at that EXT value from the TOF vs EXT plots for an entire data set (all doses and strains) on a given day. As an additional quality-control criterion, measurements that were less than the mean measurement of the previous day minus one standard deviation (which would represent negative growth) were deleted. EXT values were normalized to the control nematodes of a given strain since some strains grow more slowly than N2. We used R (SAS institute) to carry out data plotting and the nonparametric Wilcoxon rank sum test, with $p < 0.05$ considered statistically significant.

RESULTS AND DISCUSSION

Characterization of Ag NPs. Toxicity experiments were performed for 7 different Ag NPs. Except for PVP_S and PVP_L, all nanomaterials were synthesized in our laboratory. All of the tested Ag NPs were composed of Ag^0, roughly spherical and polydisperse in purified water (Figure S3). Monomer diameters (mean particle size ± standard deviation; median with 10th and 90th percentiles) were measured by ImageJ from TEM images ($n \geq 100$) and are shown in Table 1.

Dependence of Toxicity on Medium Type. As indicated in Table 1, Ag NP toxicity in the moderately hard reconstituted water ("EPA water") was higher than in K^+ medium, which has a much higher ionic strength. Control measurements were made in EPA water and K^+ medium, and when the two control groups were observed at the same experimental trial, there was no detectable difference between them. Toxicity was measured as growth inhibition over a 3-day period, with size on each day quantified as the optical density (extinction, "EXT") of the nematodes, using a COPAS BioSort. We calculated the dose of Ag NPs causing 50% growth inhibition (EC_{50}) compared to the control with no silver treatment (Figure S4), and the "threshold lethal dose" corresponding to the lowest observed concentration of Ag NPs leading to 100% mortality of nematodes within 24 h. The EC_{50} values and threshold lethal doses for each nanomaterial were 1.5 to 12 times greater in K^+ medium than in EPA water. For the dissolved $AgNO_3$ treatment, the EC_{50} value and threshold lethal dose were 100 times greater in K^+ medium than in EPA water. K^+ medium has 1600 times more chloride content than EPA water and 10 and 3.5 times the level of Ca^{2+} and Mg^{2+}, respectively. Differences in Cl^-, Ca^{2+}, Mg^{2+}, and HCO_3^{2-} levels can affect dissolution and alter the electrostatic surface properties of Ag NPs, which can affect the aggregation state of the particles in suspension.[17,37,54] Furthermore, counterions such as chloride are capable of binding Ag^+ to form aqueous Ag-chloride complexes, some of which are less bioavailable to the organisms.[55] These differences likely explain the fact that Ag NP toxicity was significantly higher in

Table 1. Mean Size of Silver Nanoparticle Monomers As Determined by Transmission Electron Microscopy and 50% Growth Inhibition Doses (EC_{50}) (in Wild Type) and Threshold Lethal Dose (Minimum Observed Dose Causing 100% Lethality within 24 h) of Tested Ag NPs and $AgNO_3$ in K^+ Medium and EPA Water

surface coatings	mean particle size ± SD (nm)	median particle size (10th, 90th percentile) (nm)	EC_{50}/μM (ppm ± SD)		threshold lethal dose/μM (ppm)	
			K^+	EPA	K^+	EPA
$AgNO_3$	N/A	N/A	59 (10)	0.6 (0.1 ± 0.02)	>59 (10)	0.9 (0.15)
PVP_8	8 ± 2	8 (2.6, 12)	13 (1.4 ± 0.3)	8 (0.9 ± 0.2)	111 (12)	9.3 (1)
PVP_{38}	38 ± 8	38 (25, 51)	17 (1.8 ± 0.5)	3.5 (0.4 ± 0.1)	111 (12)	9.3 (1)
PVP_S (NanoAmor)	21 ± 17	13 (6, 40)	463 (50)	40 (4.3)	>463 (50)	93 (10)
PVP_L (NanoAmor)	75 ± 21	76 (48, 102)	417 (45)	108 (11.7)	>463 (50)	186 (20)
CIT_7	7 ± 11	3 (1.5, 21.5)	369 (40)	31 (3.3 ± 0.7)	>463 (50)	74 (8)
GA_5	5 ± 2	5 (3.4, 7.6)	8 (0.9 ± 0.1)	0.9 (0.09 ± 0.02)	33 (3.6)	1.1 (0.1)
GA_{22}	22 ± 6	22 (15, 31)	14 (1.5 ± 0.2)	2.7 (0.3 ± 0.1)	38 (4.1)	3.9 (0.4)

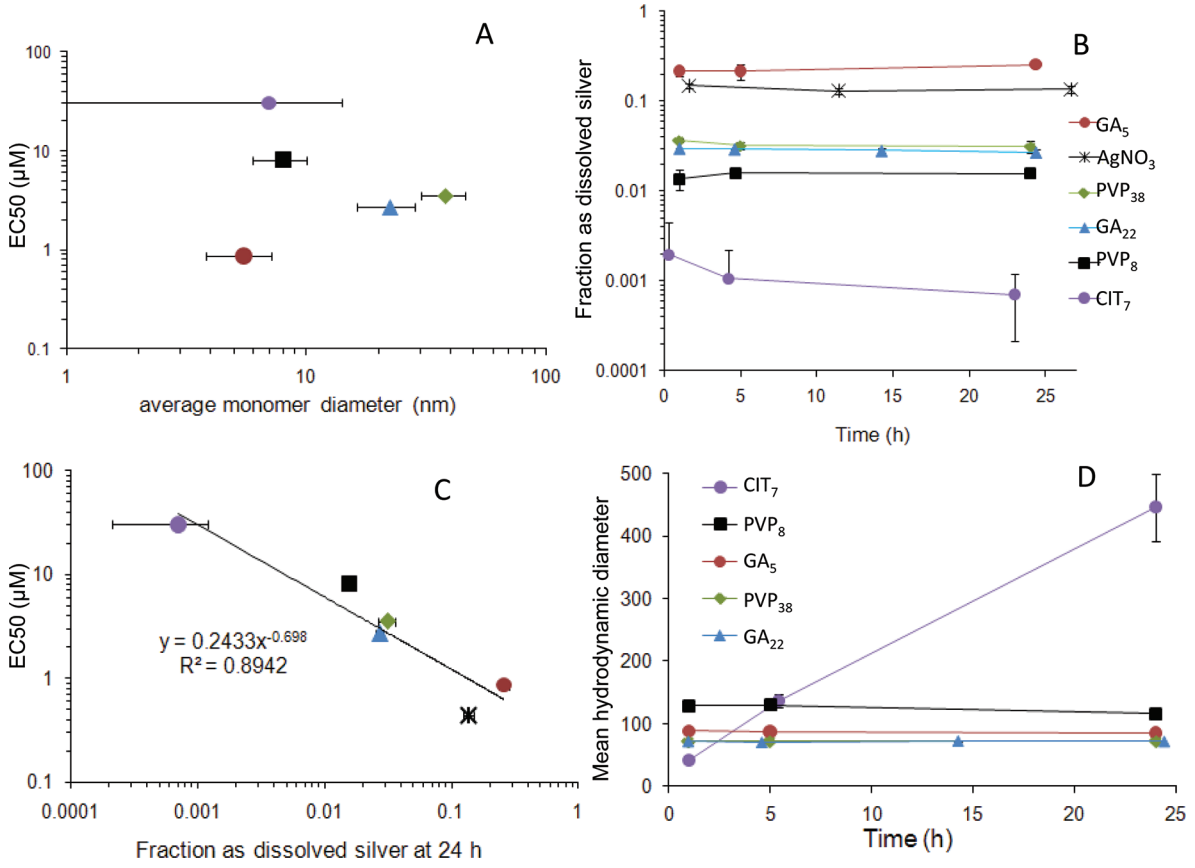

Figure 1. A) No relationship observed between the 50% effect concentration (EC_{50}) and the diameter of the Ag NP monomers. (B) Fraction of total silver passing through a 0.025 μm filter after the silver nanoparticles and $AgNO_3$ were mixed in EPA water for up to one day. The total silver concentration was different for each type of silver and ranged from 30 to 50 μM. (C) Correlation between EC_{50} values of the silver treatments and the fraction of the total silver that was dissolved at 24 h. D) Average light intensity-weighted hydrodynamic diameters of silver nanoparticles in EPA water. Data points represent the average ±1 standard deviation of replicates (n = 3). The error bars corresponding to the EC_{50} values are smaller than the symbols.

EPA water than K^+ medium for all Ag NPs. Our subsequent mechanistic analyses were carried out in EPA water.

Dependence of Toxicity on Dissolved Ag and Independence from Size or Surface Charge. Particle size may affect not only oxidative release of dissolved silver from Ag NPs[56,57] but also Ag NP reactivity due to a higher mass-normalized rate constant of surface ROS generation in nanosize than microsize particles.[26,27,58] These effects result from the increase of the specific surface area of the particles when their sizes decrease.[59,60] Other researchers have reported that smaller particles (measured by TEM) were more toxic on a mass basis than larger particles that were otherwise similar,[26,61] a generalization that did not hold entirely in our experiments, even with particles of the same coating (Figure 1A). For instance, PVP_8 had a smaller monomer size and lower ζ-potential than PVP_{38}, characteristics that, based on work with microbes, would point to higher toxicity for PVP_8.[62] However, we found that PVP_{38} was twice as toxic as PVP_8 in EPA water. Overall, while ζ-potentials were all negative with the different particle sizes and coatings (Figure S5), there was no obvious correlation between

dx.doi.org/10.1021/es202417t | Environ. Sci. Technol. 2012, 46, 1119–1127

ζ-potential and toxicity. Rather, our data suggested that other factors contributed to toxicity, particularly fraction dissolved silver (defined as the amount of silver in solution after filtration with a 0.025 μm filter) (Figures 1B and 1C). There was a clear inverse linear relationship (r^2 = 0.89) between dissolved silver and toxicity (Figure 1C), with GA_5 being the most toxic Ag NP with the highest dissolved silver concentration (comparable to $AgNO_3$), and CIT_7 being the least toxic with the lowest dissolved silver. The same relationship was observed when dissolved silver concentration rather than fraction dissolved silver after 24 h was plotted on the *x* axis (r^2 = 0.81). The dissolved silver associated with PVP_{38} in EPA water was twice that of PVP_8 (with the same initial total silver concentration) (Figure 1B). Therefore, smaller particle size was not necessarily correlated with more dissolved silver, but the dissolved silver concentration at 24 h was directly linked to differences in toxicity (Figure 1C). For GA-coated Ag NPs, suspensions with the smaller particles had much higher dissolved silver concentration (25.7% of the total silver) than the suspensions with the larger GA-coated Ag NPs (2.7% of the total silver was dissolved) (Figure 1B). Moreover, the fraction of dissolved silver in the $AgNO_3$ treatment was similar to the GA_5 suspension possibly due to supersaturation and precipitation of cerargyrite $AgCl_{(s)}$ when $AgNO_3$ was added to EPA water at concentrations greater than 5 μM (see speciation calculations in Figure S6). PVP_8 and CIT_7 particles contained only 1.6% and 0.1% dissolved silver, respectively, and were less toxic than the other silver treatments.

The average hydrodynamic diameters measured in all Ag NP suspensions were larger than the monomer diameters recorded by TEM, indicating that the Ag NPs were aggregated when they were suspended in EPA water. There was some correlation between aggregation and toxicity, with the least toxic Ag NP (CIT_7) also aggregating during the course of the exposure period (Figure 1D). Thus the reduced toxicity of CIT_7 Ag NP may be attributable to the formation of aggregates and a subsequent decrease of available surface area for dissolution. However, since there was no measurable aggregation of the other particles, it was not possible to formally correlate the aggregation state with toxicity. In addition, there is uncertainty regarding the importance of aggregation and settling in determining exposure in the context of an organism such as *C. elegans* that feeds on bacteria and large particles that have settled to the bottom of the water column and processes food by pharyngeal grinding.

Coating Effects on Dissolution and Toxicity. The smallest Ag NPs (CIT_7, PVP_8, and GA_5) were similar in size, with mean monomer diameters of <10 nm, yet were not similar in degree of toxicity: GA_5 was ∼9-fold more toxic than PVP_8, which in turn was ∼3-fold more toxic than CIT_7. Because the sizes were so similar, we attribute the difference in toxicity to surface coating. As discussed previously, this may relate in part to dissolution (Figure 1B). In addition, we hypothesized that the citrate used as a coating in the CIT_7 Ag NPs might be protective via chelation that might reduce availability of dissolved silver. We assessed this possibility via speciation modeling and toxicity testing.

First, we measured the amount of free citrate present in a filtered CIT_7 stock and found that it comprised up to 10.8 ± 0.7 mmol free citrate per mmol of total Ag. Next, we modeled the effect that this amount of citrate would have on silver speciation (Supplemental Data File 1 and Figure S6), and found that citrate significantly altered dissolved Ag(I) speciation, depending on relative proportions of dissolved Ag and citrate in EPA water.

To empirically test the importance of Ag ion and citrate in CIT_7 toxicity, we coexposed CIT_7 (37.04 μM) with $AgNO_3$ (1.18 μM). If the toxicity of CIT_7 were only driven by Ag ion, we would expect that the addition of $AgNO_3$ would increase toxicity. However, the combined toxicity was not statistically distinguishable from CIT_7 alone (data not shown). Based on our measurements of silver solubility of CIT_7 in EPA water (Figure 1B) and free citrate, we estimated that the mixture contained 1.2 μM dissolved Ag and 400 μM dissolved citrate. Our speciation calculations supported the notion that free citrate complexed a large portion (42%) of dissolved Ag (Figure S6), which would partly explain the reduction of toxicity. Another reaction that could play a role but was not captured by our equilibrium calculations is sorption of Ag ions on citrate-coated particles, which might also lead to reduced bioavailability.

Pharmacological Rescue of Ag NP Toxicity. Our dissolved silver measurements supported a dominant role for ionic silver release as the mechanism for toxicity for many Ag NPs. Next we tested whether pharmacological rescue experiments would support that result. Bioavailability of ionic silver can be reduced by binding to glutathione (GSH) or thiol-containing proteins such as metallothionein.[63] We tested the ability of a chelating chemical (N-acetyl cysteine, NAC) and an ROS-scavenging chemical (trolox) to rescue the toxicity of Ag NPs. In addition to its role as a Ag^+ chelator, NAC can also serve as an antioxidant. The concentrations of the rescue agents (61.3 μM NAC and 23 μM trolox) were chosen based on pilot studies that identified concentrations that were effective but showed no adverse effect when administered alone. The NAC molar concentration was in excess of the molar concentration of the silver, even assuming complete dissolution.

Rescue was tested in wild-type (N2 strain) nematodes, using the EC_{50} of each Ag NP. NAC completely rescued the growth inhibition of all the tested Ag NPs and $AgNO_3$. In contrast, partial rescue by trolox was observed in the following order of effect: CIT_7 > PVP_{38} > GA_{22}, and no rescue by trolox was observed for PVP_8, GA_5, or $AgNO_3$ (Figures 2A, 2B, 2E). The trolox-mediated rescue of CIT_7 toxicity was only slightly less than that of NAC. Trolox or NAC alone had no effect on nematode growth compared to controls.

Physicochemical Identification of an Effect of NAC and Trolox on Dissolution, Aggregation, and Ion Chelation but not Surface Properties. The addition of NAC to NP suspensions increased the dissolved silver concentrations, by more than 10-fold in some cases (compare Figure S7A to Figure 1B). However, chemical equilibrium calculations of Ag(+I) speciation in the EPA water matrix (refer to Supplemental Data File 1 for details) indicated that in a mixture of 30 μM NAC and dissolved Ag(+I) (ranging from 0.01 to 10 μM), Ag-NAC complexes dominated dissolved Ag(+I) speciation (Figure S6). We believe that the dominance of Ag-NAC species is applicable to our filtered Ag NP suspensions amended with NAC, in which the measured dissolved NAC concentrations were 91 to 120 μM and exceeded the silver concentrations (Figures S1 and S7A). One potential confounding factor for our NAC rescue experiments would be sorption of NAC to the Ag nanoparticles. To explore the potential for NAC-Ag NP interaction, we measured both the hydrodynamic diameter (Figure S7B) and ζ-potential of all Ag NPs with and without NAC (Figure S5). No significant changes in electrophoretic mobility (and ζ-potential) were detected (Figures S5A and S5B). Furthermore, the addition

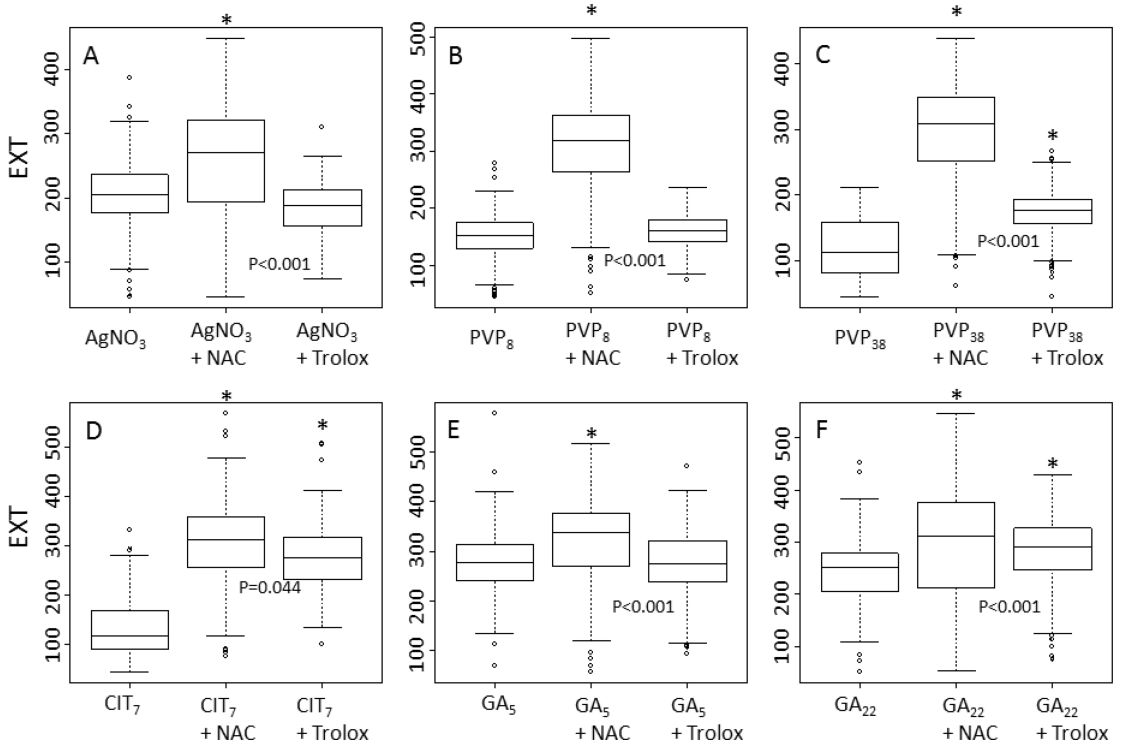

Figure 2. Pharmacological rescue of silver nanoparticle-toxicity from the addition of 61.5 μM NAC and 23 μM trolox in suspensions that contained total silver corresponding to EC_{50} values. Boxplots show the 10%, 25%, median, 75%, and 90% quantiles of EXT (extinction; a proxy for nematode size) values 72 h post exposure. Asterisks indicate statistically significant differences compared to the Ag NPs alone. A) 0.6 μM $AgNO_3$ as a positive control; B) 37 μM (total silver) citrate-coated Ag NPs; C) 4.6 μM PVP_8; D) 4.6 μM PVP_{38}; E) 0.8 μM GA_5; F) 2.8 μM GA_{22}. Rescue by trolox is an indicator of the biological effects caused by reactive oxygen species (ROS), while rescue by NAC indicates the effects were caused by ROS and/or ionic silver. The data points are combined from 3 to 4 replicate experiments.

of NAC did not change the average hydrodynamic diameter of most Ag NPs. The exceptions were CIT_7 and PVP_8. NAC reduced the aggregation rate of CIT_7 (compare Figure S7B to Figure 1D), possibly due to adsorption of NAC on Ag NP surfaces, based on the fact that less dissolved NAC was measured in the CIT_7 Ag NP suspensions compared to other Ag NPs (Figure S1). The addition of NAC to the PVP_8 suspensions resulted in the opposite effect, causing aggregation of the nanoparticles (compare Figure S7B to Figure 1D), although the reasons for this are not clear. Overall, the effects of NAC on toxicity were best explained by chelation of Ag^+ and the reduction of bioavailable forms of silver. This interpretation is supported empirically by the fact that NAC completely rescued $AgNO_3$ toxicity (Figure 2A).

Trolox is a polycarboxylate compound that can potentially bind Ag^+ ions in solution. Binding constants were not found in the literature or thermodynamic databases, so we could not directly calculate the potential for silver binding by trolox. However, if another polycarboxylate ligand, citrate, was used to estimate potential binding of Ag^+ by trolox, then the presence of 23 μM citrate (the concentration of trolox in rescue experiments) was not sufficient to alter dissolved silver speciation (Figure S6). Our model predicted that the trolox added in our rescue experiments did not affect silver speciation and only served as a ROS scavenger. This prediction was consistent with our result that trolox could not rescue $AgNO_3$ toxicity (Figure 2A).

Analysis of the Mechanism of Ag NP Toxicity via Genetic Approaches. We further tested mechanisms of Ag NP toxicity with a third set of experiments comparing the effects of different Ag NPs on mutant and wild-type (N2) nematodes. This genetic approach was based on the toxicological importance of specific genes in mediating the vulnerability to Ag NPs. For example, nematodes lacking DNA repair capacity are more vulnerable than N2 nematodes to exposures that cause DNA damage.[45,64] Since we wished to test the roles of oxidative stress and metal ions in mediating toxicity, we chose two oxidant-sensitive (*sod-3* and *mev-1*) and two metal-sensitive (*mtl-2* and *pcs-1*) mutants. The *mev-1* mutant carries a mutation in a succinate dehydrogenase subunit that renders it highly susceptible to oxidative stress.[65,66] The *sod-3* nematodes are deficient in one of the two *C. elegans* mitochondrial superoxide dismutases and are oxidative stress-sensitive.[67] The *mtl-2* strain lacks one of the two metallothionein genes and is sensitive to multiple metals.[68−70] The *pcs-1* nematodes lack phytochelatin synthase, an enzyme that synthesizes a poly glutathione cysteine-rich peptide with strong metal-chelating capacity, and are more sensitive than *mtl-2* mutants to many metals.[71]

We selected doses for the more toxic Ag NPs (PVP_8, PVP_{38}, CIT_7, GA_5, and GA_{22}) at which an intermediate level of growth inhibition (30−50%) was induced in N2s, such that increased susceptibility in mutant strains would be detectable if present. Metal-chelating mutants were more sensitive to ionic silver and all Ag NPs (Table 2), while oxidative stress-sensitive mutants were more sensitive only to PVP_{38}, CIT_7, and GA_{22} (Figure S8).

Combined mutant and pharmacological rescue analysis confirms the role of Ag^+ in CIT_7 toxicity. While our mutant experiments supported a role for Ag ions in CIT_7 Ag NP toxicity, our pharmacological rescue results were equivocal: the difference in rescue by trolox and NAC was small and statistically marginal ($p = 0.044$, compared to $p < 0.001$ for all

Table 2. Mutant Sensitivity Analysis of All Ag NPs and $AgNO_3$[a]

strain sensitivity	N2	mtl-2	pcs-1	mev-1	sod-3
$AgNO_3$	+	++	++	+	+
PVP_8	+	++	++	+	+
PVP_{38}	+	++	++	++	++
CIT_7	+	++	++	++	++
GA_5	+	++	++	+	+
GA_{22}	+	++	++	++	++

[a]"+" indicates basal sensitivity of N2s, and "++" indicates increased sensitivity.

other Ag NPs). To further confirm the Ag ion-mediated effect in CIT_7 toxicity, we used the metal ion-sensitive mutant *pcs-1* to test its pharmacological rescue. Since *pcs-1* was the most susceptible strain tested, we reduced the dosing concentration of CIT_7 to 18.5 μM (compared to 37 μM in N2s). Most nematodes died by 24 h post exposure, while no mortality was observed when nematodes were coexposed with either trolox (23 μM) or NAC (61.3 μM). However, trolox only rescued mortality but not growth, so the nematodes arrested at the L_2 stage, while NAC not only rescued mortality but also restored nematode growth to control levels (Figure S9). Thus, CIT_7 Ag NPs do exert toxicity via release of ions, although this effect is less important than for PVP_8, PVP_{38}, GA_5, and GA_{22} Ag NPs.

Complexation of Silver Ions in Our Experimental Conditions. All of the experiments described so far suggest that the most toxic Ag NPs were also the most soluble and therefore likely acted largely by releasing silver ions that bind to sulfhydryl groups associated with proteins and low molecular weight antioxidants such as glutathione. In contrast, the less-soluble Ag NPs also caused toxicity via oxidative stress. This pattern predicts that we should see a great deal of thiol binding of silver inside the *C. elegans* upon incubation of $AgNO_3$. To test this hypothesis, we measured silver speciation through Ag K-edge XANES analysis on washed *C. elegans* individuals (or their bacterial food source) after they were incubated with $AgNO_3$. The shape of the XANES spectra and the position of the edge are distinguishable for AgCl, Ag_2O, $AgNO_3$, or Ag_2S compounds. Consequently, a change in the silver ions speciation after incubation with the nematodes or their food can be quantified using linear combination fitting (LCF) of reference compounds. Obvious differences (a strong decrease of the white line intensity) are observed in the XANES spectra of the $AgNO_3$ after interaction with the organisms. Using LCF, we conclude that 89 to 96% of the silver is complexed with sulfur atoms *in vivo* while silver atoms are only surrounded by oxygen atoms before incubation (Figure S10).

Further Implications. The mechanism of Ag NP toxicity was dependent in these experiments on dissolved silver and surface coating. Three independent lines of evidence demonstrated that release of Ag^+ contributed to the toxicity for all the tested Ag NPs and was a major driver for the toxicity of many, including the most toxic (GA_5). A role for oxidative stress, presumably "nano-specific" generation of reactive oxygen species, was also supported but only in the cases of larger or less toxic Ag NPs (PVP_{38}, CIT_7, and GA_{22}; Table 1), which were generally less soluble. These results demonstrated that both mechanisms of toxicity (dissolved Ag^+ and oxidative stress) can occur with Ag NPs; however, in our experiments, the ROS mechanism was apparent only when dissolved silver is minimal. Our findings may explain the differing literature reports on the role of oxidative stress in Ag NP toxicity. Of note, while silver ion could in principle cause indirect oxidative stress via depletion of biological thiols such as glutathione,[72] this was not a major mode of toxicity of silver ion in our experiments, as demonstrated both by the inability of trolox to rescue $AgNO_3$ toxicity (Figure 2A) and by the lack of sensitivity to $AgNO_3$ of the *mev-1* and *sod-3* strains (Table 2). Based on our EPA water results, the toxicity of Ag NPs could be conservatively estimated as no greater than the toxicity of an equivalent mass of dissolved silver. However, there were exceptions to this in K^+ medium (where overall toxicity was less), and other reports have identified greater toxicity associated with nanoparticulate Ag.[26−30,40,70,73] It will be important to elucidate the reason for these differences. It is interesting to note that most studies that report that Ag NPs are more toxic than the equivalent mass of dissolved silver or that generation of reactive oxygen species is a major driver for toxicity, are carried out in single-cell systems (either microbial or cell culture experiments),[26−30,74] with some exceptions.[42,75] On the other hand, most studies that report that Ag NPs cause toxicity largely via dissolution have been carried out in multicellular organisms.[8,12,17]

■ ASSOCIATED CONTENT

Supporting Information

Two supplemental data files and eleven supplemental figures. This material is available free of charge via the Internet at http://pubs.acs.org.

■ AUTHOR INFORMATION

Corresponding Author

*Phone: + 919 613 8109. Fax: + 919 668 1799. E-mail: joel.meyer@duke.edu.

■ ACKNOWLEDGMENTS

This work was supported by the National Science Foundation (NSF) and the Environmental Protection Agency (EPA) under NSF Cooperative Agreement EF-0830093, Center for the Environmental Implications of NanoTechnology (CEINT). Any opinions, findings, conclusions or recommendations expressed in this material are those of the author(s) and do not necessarily reflect the views of the NSF or the EPA. This work has not been subjected to EPA review and no official endorsement should be inferred. Strain VC433 was provided by the *C. elegans* Reverse Genetics Core Facility at UBC, which is part of the International *C. elegans* Gene Knockout Consortium. A.G. was also supported by the Greek Scholarship Foundation. We gratefully acknowledge Elena Turner for experimental assistance, Appala R. Badireddy for helping with sample processing in the XAS studies, Yingwen Cheng for GA-coated Ag NP synthesis, Kevin Kwok in experimental design, and FAME beamline operators (especially Olivier Proux) at the European Synchrotron Radiation Facility. We also thank Amanda Bess for her detailed draft review and Jason Unrine for his experimental design suggestions.

■ REFERENCES

(1) Chen, X.; Schluesener, H. J. Nanosilver: A nanoproduct in medical application. *Toxicol. Lett.* **2008**, *176* (1), 1−12.

(2) Ahamed, M.; Alsalhi, M. S.; Siddiqui, M. K. Silver nanoparticle applications and human health. *Clin. Chim. Acta* **2010**.

(3) Benn, T. M.; Westerhoff, P. Nanoparticle silver released into water from commercially available sock fabrics. *Environ. Sci. Technol.* **2008**, *42* (11), 4133−4139.

(4) Bryaskova, R.; et al. Antibacterial activity of poly(vinyl alcohol)-b-poly(acrylonitrile) based micelles loaded with silver nanoparticles. *J. Colloid Interface Sci.* **2010**, *344* (2), 424−428.
(5) Lara, H. H.; et al. Bactericidal effect of silver nanoparticles against multidrug-resistant bacteria. *World J. Microbiol. Biotechnol.* **2010**, *26* (4), 615−621.
(6) Lee, S. M.; Song, K. C.; Lee, B. S. Antibacterial activity of silver nanoparticles prepared by a chemical reduction method. *Korean J. Chem. Eng.* **2010**, *27* (2), 688−692.
(7) Li, W. R.; et al. Antibacterial activity and mechanism of silver nanoparticles on Escherichia coli. *Appl. Microbiol. Biotechnol.* **2010**, *85* (4), 1115−1122.
(8) Bar-Ilan, O.; et al. Toxicity Assessments of Multisized Gold and Silver Nanoparticles in Zebrafish Embryos. *Small* **2009**, *5* (16), 1897−1910.
(9) Asharani, P. V.; et al. Toxicity of silver nanoparticles in zebrafish models. *Nanotechnology* **2008**, *19* (25), 1−8.
(10) Lee, K. J.; et al. In vivo imaging of transport and biocompatibility of single silver nanoparticles in early development of zebrafish embryos. *ACS Nano* **2007**, *1* (2), 133−143.
(11) Chae, Y. J.; et al. Evaluation of the toxic impact of silver nanoparticles on Japanese medaka (Oryzias latipes). *Aquat. Toxicol.* **2009**, *94* (4), 320−327.
(12) Bilberg, K.; et al. Silver nanoparticles and silver nitrate cause respiratory stress in Eurasian perch (Perca fluviatilis). *Aquat. Toxicol.* **2010**, *96* (2), 159−165.
(13) AshaRani, P. V.; Hande, M. P.; Valiyaveettil, S. Anti-proliferative activity of silver nanoparticles. *BMC Cell Biol.* **2009**, *10*, 65.
(14) Chen, D. F.; Xi, T. F.; Bai, J. Biological effects induced by nanosilver particles: in vivo study. *Biomed. Mater. (Bristol, U. K.)* **2007**, *2* (3), S126−S128.
(15) Rahman, M. F.; et al. Expression of genes related to oxidative stress in the mouse brain after exposure to silver-25 nanoparticles. *Toxicol. Lett.* **2009**, *187* (1), 15−21.
(16) Roh, J. Y.; et al. Ecotoxicity of Silver Nanoparticles on the Soil Nematode *Caenorhabditis elegans* Using Functional Ecotoxicogenomics. *Environ. Sci. Technol.* **2009**, *43* (10), 3933−3940.
(17) Meyer, J. N.; et al. Intracellular uptake and associated toxicity of silver nanoparticles in *Caenorhabditis elegans*. *Aquat. Toxicol.* **2010**, *100* (2), 140−50.
(18) Wiesner, M. R.; et al. Decreasing Uncertainties in Assessing Environmental Exposure, Risk, and Ecological Implications of Nanomaterials. *Environ. Sci. Technol.* **2009**, *43* (17), 6458−6462.
(19) Auffan, M.; et al. Inorganic manufactured nanoparticles: how their physicochemical properties influence their biological effects in aqueous environments. *Nanomedicine* **2010**, *5* (6), 999−1007.
(20) Liu, J.; Hurt, R. H. Ion Release Kinetics and Particle Persistence in Aqueous Nano-Silver Colloids. *Environ. Sci. Technol.* **2010**, *44* (6), 2169−2175.
(21) Kvitek, L.; et al. Initial Study on the Toxicity of Silver Nanoparticles (NPs) against Paramecium caudatum. *J. Phys. Chem. C* **2009**, *113* (11), 4296−4300.
(22) Kittler, S.; et al. Synthesis of PVP-coated silver nanoparticles and their biological activity towards human mesenchymal stem cells. *Materialwiss. Werkstofftech.* **2009**, *40* (4), 258−264.
(23) Miao, A. J.; et al. The algal toxicity of silver engineered nanoparticles and detoxification by exopolymeric substances. *Environ. Pollut.* **2009**, *157* (11), 3034−3041.
(24) Navarro, E.; et al. Toxicity of Silver Nanoparticles to *Chlamydomonas reinhardtii*. *Environ. Sci. Technol.* **2008**, *42* (23), 8959−8964.
(25) Xiu, Z. M.; Ma, J.; Alvarez, P. J. Differential Effect of Common Ligands and Molecular Oxygen on Antimicrobial Activity of Silver Nanoparticles versus Silver Ions. *Environ. Sci. Technol.* **2011**, *45*, 9003−9008.
(26) Carlson, C.; et al. Unique Cellular Interaction of Silver Nanoparticles: Size-Dependent Generation of Reactive Oxygen Species. *J. Phys. Chem. B* **2008**, *112* (43), 13608−13619.
(27) Choi, O.; Hu, Z. Q. Size dependent and reactive oxygen species related nanosilver toxicity to nitrifying bacteria. *Environ. Sci. Technol.* **2008**, *42* (12), 4583−4588.
(28) Kim, S.; et al. Oxidative stress-dependent toxicity of silver nanoparticles in human hepatoma cells. *Toxicol. in Vitro* **2009**, *23* (6), 1076−1084.
(29) Foldbjerg, R.; et al. PVP-coated silver nanoparticles and silver ions induce reactive oxygen species, apoptosis and necrosis in THP-1 monocytes. *Toxicol. Lett.* **2009**, *190* (2), 156−162.
(30) AshaRani, P. V.; et al. Cytotoxicity and Genotoxicity of Silver Nanoparticles in Human Cells. *ACS Nano* **2009**, *3* (2), 279−290.
(31) Kawata, K.; Osawa, M.; Okabe, S. In Vitro Toxicity of Silver Nanoparticles at Noncytotoxic Doses to HepG2 Human Hepatoma Cells. *Environ. Sci. Technol.* **2009**, *43* (15), 6046−6051.
(32) Eom, H.-J.; Choi, J. p38 MAPK Activation, DNA Damage, Cell Cycle Arrest and Apoptosis As Mechanisms of Toxicity of Silver Nanoparticles in Jurkat T Cells. *Environ. Sci. Technol.* **2010**, *44* (21), 8337−8342.
(33) Kittler, S.; et al. Synthesis of PVP-coated silver nanoparticles and their biological activity towards human mesenchymal stem cells. *Materialwiss. Werkstofftech.* **2009**, *40* (4), 258−264.
(34) Liu, F.; et al. Ultrathin Diamond-like Carbon Film Coated Silver Nanoparticles-Based Substrates for Surface-Enhanced Raman Spectroscopy. *ACS Nano* **2010**, *4* (5), 2643−2648.
(35) Lu, W. T.; et al. Effect of surface coating on the toxicity of silver nanomaterials on human skin keratinocytes. *Chem. Phys. Lett.* **2010**, *487* (1−3), 92−96.
(36) Suresh, A. K.; et al. Silver Nanocrystallites: Biofabrication using *Shewanella oneidensis*, and an Evaluation of Their Comparative Toxicity on Gram-negative and Gram-positive Bacteria. *Environ. Sci. Technol.* **2010**, *44* (13), 5210−5215.
(37) Jin, X.; et al. High-Throughput Screening of Silver Nanoparticle Stability and Bacterial Inactivation in Aquatic Media: Influence of Specific Ions. *Environ. Sci. Technol.* **2010**, *44* (19), 7321−7328.
(38) Muhling, M.; et al. Impact of Silver Nanoparticle Contamination on the Genetic Diversity of Natural Bacterial Assemblages in Estuarine Sediments. *Environ. Sci. Technol.* **2009**, *43* (12), 4530−4536.
(39) Kennedy, A. J.; et al. Fractionating Nanosilver: Importance for Determining Toxicity to Aquatic Test Organisms. *Environ. Sci. Technol.* **2010**, *44* (24), 9571−9577.
(40) Damm, C.; Munstedt, H. Kinetic aspects of the silver ion release from antimicrobial polyamide/silver nanocomposites. *Appl. Phys. A: Mater. Sci. Process.* **2008**, *91* (3), 479−486.
(41) Williams, P. L.; Dusenbery, D. B. Using the Nematode *Caenorhabditis-Elegans* to Predict Mammalian Acute Lethality to Metallic Salts. *Toxicol. Ind. Health* **1988**, *4* (4), 469−478.
(42) Yin, L.; et al. More than the Ions: The Effects of Silver Nanoparticles on Lolium multiflorum. *Environ. Sci. Technol.* **2011**, *45* (6), 2360−2367.
(43) Silvert, P.-Y.; et al. Preparation of colloidal silver dispersions by the polyol process. Part 1-Synthesis and characterization. *J. Mater. Chem.* **1996**, *6* (4), 573−577.
(44) Silvert, P.-Y.; Herrera-Urbina, R.; Tekaia-Elhsissen, K. Preparation of colloidal silver dispersions by the polyol process. *J. Mater. Chem.* **1997**, *7* (2), 293−299.
(45) Leung, M. C.; et al. *Caenorhabditis elegans* Generates Biologically Relevant Levels of Genotoxic Metabolites from Aflatoxin B1 but Not Benzo[a]pyrene In Vivo. *Toxicol. Sci.* **2010**, *118* (2), 444−453.
(46) *Particle deposition and aggregation: measurement, modelling and simulation;* Elimelech, M. J. G., Xiadong, J.,Williams, R., Eds.; 1998; pp 27−29.
(47) Vairavamurthy, A.; Mopper, K. Field methods for determination of traces of thiols in natural waters. *Anal. Chim. Acta* **1990**, *236*, 363−370.
(48) Hsu-Kim, H. Stability of metal - glutathione complexes during oxidation by hydrogen peroxide and Cu(II) catalysis. *Environ. Sci. Technol.* **2007**, *41*, 2338−2342.

(49) Proux, O.; et al. FAME: a new beamline for x-ray absorption investigations of very-diluted systems of environmental, material and biological interests. *Phys. Scr.* **2005**, *2005* (T115), 970.
(50) Proux, O.; et al. Feedback system of a liquid-nitrogen-cooled double-crystal monochromator: design and performances. *J. Synchrotron Radiat.* **2006**, *13* (Pt 1), 59−68.
(51) Ravel, B.; Newville, M. ATHENA, ARTEMIS, HEPHAESTUS: data analysis for X-ray absorption spectroscopy using IFEFFIT. *J. Synchrotron Radiat.* **2005**, *12*, 537−541.
(52) Pulak, R. Techniques for analysis, sorting, and dispensing of C. elegans on the COPAS flow-sorting system. *Methods Mol. Biol.* **2006**, *351*, 275−86.
(53) Smith, M. V.; et al. A Discrete Time Model for the Analysis of Medium-Throughput C. elegans Growth Data. *PLoS One* **2009**, *4* (9), e7018.
(54) Li, X. A.; Lenhart, J. J.; Walker, H. W. Dissolution-Accompanied Aggregation Kinetics of Silver Nanoparticles. *Langmuir* **2010**, *26* (22), 16690−16698.
(55) Lead, J. R.; et al. Silver nanoparticles: Behaviour and effects in the aquatic environment. *Environ. Int.* **2011**, *37* (2), 517−531.
(56) Elzey, S.; Grassian, V. H. Agglomeration, isolation and dissolution of commercially manufactured silver nanoparticles in aqueous environments. *J. Nanopart. Res.* **2010**, *12* (5), 1945−1958.
(57) Liu, J.; et al. Controlled Release of Biologically Active Silver from Nanosilver Surfaces. *ACS Nano* **2010**, 6903−6913.
(58) Nurmi, J. T.; et al. Characterization and properties of metallic iron nanoparticles: Spectroscopy, electrochemistry, and kinetics. *Environ. Sci. Technol.* **2005**, *39* (5), 1221−1230.
(59) Stoeger, T.; et al. Inflammatory response to TiO2 and Carbonaceous particles scales best with BET surface area. *Environ. Health Perspect.* **2007**, *115* (6), A290−A291.
(60) Wittmaack, K. In Search of the Most Relevant Parameter for Quantifying Lung Inflammatory Response to Nanoparticle Exposure: Particle Number. Surface Area, or What? *Environ. Health Perspect.* **2006**, *115*, 2.
(61) Morones, J. R.; et al. The bactericidal effect of silver nanoparticles. *Nanotechnology* **2005**, *16* (10), 2346−2353.
(62) El Badawy, A. M.; et al. Surface Charge-Dependent Toxicity of Silver Nanoparticles. *Environ. Sci. Technol.* **2011**, *45* (1), 283−287.
(63) Kristiansen, S.; Ifversen, P.; Danscher, G. Ultrastructural localization and chemical binding of silver ions in human organotypic skin cultures. *Histochem. Cell Biol.* **2008**, *130* (1), 177−184.
(64) Boyd, W. A.; et al. Nucleotide excision repair genes are expressed at low levels and are not detectably inducible in *Caenorhabditis elegans* somatic tissues, but their function is required for normal adult life after UVC exposure. *Mutat. Res., Fundam. Mol. Mech. Mutagen.* **2010**, *683* (1−2), 57−67.
(65) Vazquez-Manrique, R. P.; et al. Reduction of *Caenorhabditis elegans* frataxin increases sensitivity to oxidative stress, reduces lifespan, and causes lethality in a mitochondrial complex II mutant. *FASEB J.* **2005**, *19* (12), 172−174.
(66) Ishii, N.; et al. A Methyl Viologen-Sensitive Mutant of the Nematode *Caenorhabditis-Elegans*. *Mutat. Res.* **1990**, *237* (3−4), 165−171.
(67) Dingley, S.; et al. Mitochondrial respiratory chain dysfunction variably increases oxidant stress in *Caenorhabditis elegans*. *Mitochondrion* **2010**, *10* (2), 125−136.
(68) Swain, S. C.; et al. C-elegans metallothioneins: New insights into the phenotypic effects of cadmium toxicosis. *J. Mol. Biol.* **2004**, *341* (4), 951−959.
(69) Jiang, G. C. T.; et al. *Caenorhabditis elegans* Metallothioneins Protect against Toxicity Induced by Depleted Uranium. *Toxicol. Sci.* **2009**, *111* (2), 345−354.
(70) Cui, Y. X.; et al. Toxicogenomic analysis of *Caenorhabditis elegans* reveals novel genes and pathways involved in the resistance to cadmium toxicity. *Genome Biol.* **2007**, *8* (6), R122.
(71) Hughes, S. L.; et al. The Metabolomic Responses of *Caenorhabditis elegans* to Cadmium Are Largely Independent of Metallothionein Status, but Dominated by Changes in Cystathionine and Phytochelatins. *J. Proteome Res.* **2009**, *8* (7), 3512−3519.
(72) Di Giulio, R. T.; Meyer, J. N. Reactive oxygen species and oxidative stress. *The Toxicology of Fishes*; ed. D.G.R.a.H. DE. Taylor and Francis: Washington, DC, 2008; pp 273−324.
(73) Hughes, S. L.; et al. The Metabolomic Responses of *Caenorhabditis elegans* to Cadmium Are Largely Independent of Metallothionein Status, but Dominated by Changes in Cystathionine and Phytochelatins. *J. Proteome Res.* **2009**, *8* (7), 3512−3519.
(74) Powers, C. M.; et al. Silver Impairs Neurodevelopment: Studies in PC12 Cells. *Environ. Health Perspect.* **2010**, *118* (1), 73−79.
(75) Powers, C. M.; et al. Silver Nanoparticles Compromise Neurodevelopment in PC12 Cells: Critical Contributions of Silver Ion, Particle Size, Coating, and Composition. *Environ. Health Perspect.* **2011**, *119* (1), 37−44.